Journal of ELECTRONIC MATERIALS, Vol. 46, No. 1, 2017
DOI: 10.1007/s11664-016-4878-6

Excellent Formaldehyde Gas-Sensing Properties of Ruptured Nd-Doped In_2O_3 Porous Nanotubes

XUESONG WANG,[1] HAIYING LI,[1] MUCUI NI,[1] LIANYUAN WANG,[1] LI LIU,[1,2,3] HAN WANG,[1] and XUEXIN GUO[1]

1.—State Key Laboratory of Superhard Materials, College of Physics, Jilin University, Changchun 130012, People's Republic of China. 2.—e-mail: liuli_teacher@163.com. 3.—e-mail: liul99@jlu.edu.cn

The ruptured Nd-doped In_2O_3 porous nanotubes have been successfully synthesized by single-capillary electrospinning method. The morphologies of the as-prepared materials were characterized by scanning electron microscopy and transmission electron microscopy. It can be seen obviously that the surface of the nanotubes are distributed with cracks and pores, which formed such an open nanostructure. The crystal structures and components were determined by x-ray diffraction, energy-dispersive x-ray spectroscopy and x-ray photoelectron spectrometer. The gas-sensing properties of ruptured Nd-doped In_2O_3 porous nanotubes were studied and the results show the excellent performances of the as-obtained materials. The response of ruptured Nd-doped In_2O_3 porous nanotubes to 100 ppm of formaldehyde is 46.8 at the optimum temperature of 240°C. The response and recovery times are 8 s and 22 s, respectively. Furthermore, the lowest detection limit of formaldehyde is 100 ppb with the value of 2.4. In addition, the ruptured Nd-doped In_2O_3 porous nanotubes exhibit good selectivity to formaldehyde and long-term stability.

Key words: Ruptured nanotubes, porous, Nd-doped In_2O_3, formaldehyde sensor

INTRODUCTION

Due to the increasing popularity of chemical products in daily life, our lives are becoming more and more comfortable and convenient. However, some negative effects have gradually emerged. For instance, some indoor fixtures can release formaldehyde gas which endangers human health. At present there are many methods to detect the existence and concentration of formaldehyde, such as spectrophotometric, colorimetric and catalytic method.[1–4] However, there are usually some disadvantages of these methods such as complicated operation and expensive cost. During the past decades, semiconducting oxides have been widely used in many fields such as photosensitization[5] and lithium storage.[6] Gas sensors based on semiconducting oxides have received widespread attention due the benefits of their easy fabrication and low cost.[7] However, there are still some drawbacks which limit the practical application of semiconducting oxide gas sensors such as low sensitivity and poor selectivity. Recently, many efforts have been made to solve these problems, and one of the most effective ways is to increase the surface-to-volume ratio.[8] Previous studies have demonstrated that porosity plays a vital role in the enhancement of the gas-sensing performance of materials, since it can improve the transport speed of gas molecules in materials and provide more effective contacts between gas and materials.[9] For instance, Wang et al.[10] synthesized porous SnO_2 carbon nanofibers by calcining at a high temperature and this exhibited good performance with carbon tetrachloride. An et al.[11] obtained porous carbon nanofibers by reducing SnO_2 using H_2. However, these methods generally have some disadvantages such as complex fabrication and high cost. Herein, we introduce a

(Received April 21, 2016; accepted August 12, 2016; published online September 12, 2016)

simple method to fabricate ruptured Nd-doped In_2O_3 porous nanotubes with cracks and pores on the surface.

In_2O_3 is an *n*-type semiconducting oxide with a wide band gap.[12] It has been studied extensively due to its advantages of non-toxicity and stability, and it can can be used as a base for doping other dopants. Rare earth elements have been widely studied in the fundamental and technical field over the past decades due to their particular characteristics arising from the 4f electronic shells.[13] However, Nd-doped In_2O_3 have never been studied in the field of gas sensors. Many studies have demonstrated that the exposure of the inner/outer surfaces of nanotubes will provide larger reactive sites, which is very crucial for their gas-sensing performance.[14] The ruptured porous nanotube structure is a more open nanostructure which provides easy pathways for gas molecules to penetrate easily into the whole nanotubes, making ruptured In_2O_3 porous nanotubes suitable candidates for use as gas sensors.[15]

In this paper, ruptured Nd-doped In_2O_3 porous nanotubes are successfully synthesized by the single nozzle electrospinning and calcination method. The gas-sensing properties of the as-obtained materials to formaldehyde are also investigated. The experiment results show that this novel ruptured nanotube structure possesses a more open structure that enhances its gas-sensing performances.

EXPERIMENTAL

Materials

All chemical reagents were of analytical grade and used without further purification. Poly(vinylpyrrolidone)—PVP, M_w = 1,300,000—was obtained from Sigma-Aldrich (USA). $In(NO_3)_3$ (99.99%), $Nd(NO_3)_3 \cdot 6H_2O$ (99.99%), N,N-dimethylformamide (DMF ≥ 99.5%), and ethanol (≥99.7%) were purchased from Aladdin (Shanghai, China).

Synthesis and Characterization of Ruptured Nd-Doped In_2O_3 Porous Nanotubes

Ruptured Nd-doped In_2O_3 porous nanotubes were synthesized via a simple single-capillary electrospinning method.[16] Briefly, 0.4 g of $In(NO_3)_3$ and 0.0358 g of $Nd(NO_3)_3 \cdot 6H_2O$ were mixed with 2.2 g of DMF and 2.2 g of ethanol. The two mixtures were under magnetic stirring at room temperature for 30 min. Then, the solution was added into 0.5 g of PVP and was stirred for 12 h. The mixture was ejected from the stainless steel capillary with a voltage of 13 kV and the distance between the capillary and collector was 25 cm. Then, the electrospinning non-woven mats were collected and annealed at a rising rate of 22°C/min from room temperature and a keeping time of 180 min at 550°C. At last, the furnace was self-cooled to room temperature. Powder x-ray diffraction (XRD) analysis was conducted using a PANalytical Empyrean diffractometer with Cu K_α radiation (λ = 1.5406 Å). Energy-dispersive x-ray (EDX) spectrometry was performed using a Hitachi S4800 system. Scanning electron microscopy (SEM) images were recorded using a Hitachi S4800 instrument. Transmission electron microscopy (TEM) images were recorded with a JEOL-2000EX. X-ray photoelectron spectroscopy (XPS) measurements were carried out on an ESCLAB KMII using Al as the exciting source.

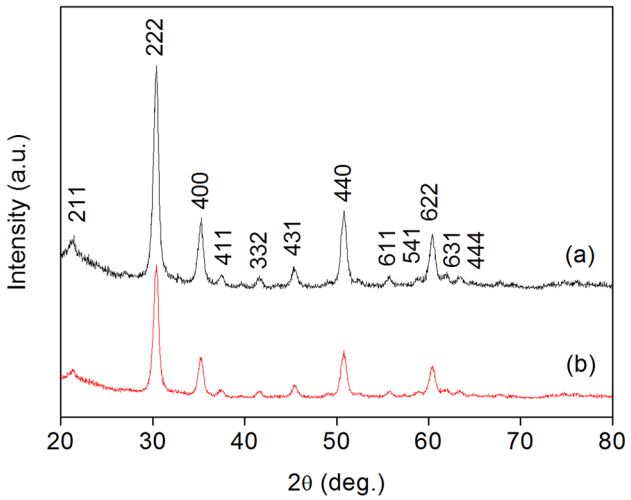

Fig. 1. XRD patterns of (a) pure and (b) Nd-doped In_2O_3 porous nanotubes.

The process of gas sensor fabrication is described in previous work.[17] In detail, a certain volume of deionized water was mixed with the samples to form a paste. Subsequently, a ceramic tube with a pair of gold electrodes was coated with the paste. A spring-like Ni–Cr wire plugged in the ceramic tube was used to provide the operating temperature. The gas sensors need to be dried in shade prior to the first measurement. The sensor response ($S = R_a/R_g$) was defined as the ratio of the sensor resistances in the air (R_a) to that in the target gas (R_g). The response time was defined as the time taken by the sensor to achieve 90% of the resistance variation, and the recovery time was the time taken by the sensor to return 90% of the resistance variation when exposed to air. The sensing properties of the sensors were measured using a CGS-8 Intelligent gas-sensing analysis system (Beijing Elite Tech Co., Ltd., Beijing, China).

RESULTS AND DISCUSSION

Structure and Morphological Characteristics

The XRD patterns of (a) pure and (b) Nd-doped In_2O_3 porous nanotubes are shown in Fig. 1. All the samples are well-crystallized and no additional impurity peaks are detected, implying the high purity of the as-synthesized materials. The diffraction peaks can be indexed to cubic In_2O_3 (JCPDS No. 71-2195).

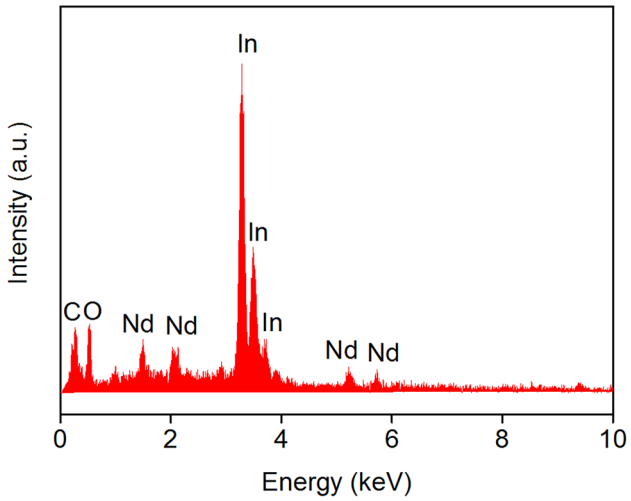

Fig. 2. EDX pattern of the ruptured Nd-doped In_2O_3 porous nanotubes.

Figure 2 displays the EDX pattern collected from the ruptured Nd-doped In_2O_3 porous nanotubes. It demonstrates that the obtained materials are composed of In, O and Nd. The peak of C is derived from the conducting resin during the measurement.

The morphologies of (a, b and c) Nd-doped and (d) pure In_2O_3 porous nanotubes are shown in Fig. 3. All the nanotubes are randomly distributed and with a uniform diameter of approximately 200 nm. Moreover, it can be clearly seen that the surface of the nanotubes is distributed with cracks and holes, which facilitate passages for diffusion throughout the whole nanotube.

Further detailed structural analysis of Nd-doped In_2O_3 porous nanotubes was carried out using TEM. Figure 4a shows the TEM image of representative Nd-doped In_2O_3 nanotubes. It can be seen that the size and shape of the product were similar to those of the SEM observations. The high-resolution transmission electron microscopy (HRTEM) image (Fig. 4b) showed a fringe distance of 0.291 nm, corresponding to the lattice distances of the (222) plane of cubic In_2O_3.[18]

Furthermore, XPS spectra are taken to investigate the chemical composition of Nd-doped In_2O_3 porous nanotubes. As shown in Fig. 5a, the double peaks located at 452 and 444.45 eV are indexed to the In $3d_{5/2}$ and In $3d_{3/2}$, respectively, which can match well with the spin–orbit split of cubic In_2O_3.[19] Figure 5b shows the Nd 3d spin–orbit doublet recorded from the XPS spectrum, which corresponds to the $3d_{3/2}$ and $3d_{5/2}$ peaks positioned around 1005.5 and 983.3 eV, respectively.[20] The result indicated that Nd ions have entered the materials.

Gas-Sensing Properties

The response curves of pure, 9 mol.%, 11 mol.%, and 13 mol.% Nd-doped In_2O_3 porous nanotube sensors to 100 ppm formaldehyde at different operating temperatures are shown in Fig. 6. The sensitivity of all the sensors increases sharply as the temperature increases and reach the maximum response at 240°C. Then the sensitivity begins to decrease when the temperature continues rising. Therefore, 240°C is defined as the optimum operating temperature. It can be seen that the sensitivity of In_2O_3 porous nanotubes has been improved after doping with Nd, and the optimal doping amount is 11 mol.%. The low sensitivity at a lower percentage of dopant is because the dopant doesn't play a major role. And the decrease in the sensitivity at a higher percentage of dopant is attributed to the decrease of the effective surface adsorption areas.[21]

The response curves of ruptured Nd-doped In_2O_3 nanotubes to different concentrations of formaldehyde at 240°C are presented in Fig. 7a. It can be seen from the inset image that the sensitivity changed almost linearly with the concentration of formaldehyde at low concentrations (0.1–100 ppm). The sensitivity did not reach saturation until a concentration of 2000 ppm, indicating the large testing scope to formaldehyde. Furthermore, the lowest detection limit is a very important factor for gas sensors in practical applications. In this experiment, even at 100 ppb of formaldehyde, the sensitivity of ruptured Nd-doped In_2O_3 porous nanotubes can still be observed and the response value is 2.4. Figure 7b displays the sensitivity of gas sensors in the range between 100 ppb and 5 ppm, which is the range of most applications. It can be seen that the Nd-doped In_2O_3 porous nanotube sensors possess good formaldehyde-sensing properties at such low concentrations.

Figure 8 displays three cycles of dynamic response and recovery curves of pure and Nd-doped In_2O_3 nanotubes to 100 ppm of formaldehyde at 240°C. It can be seen that compared to pure In_2O_3 (response value is 13.4), the sensitivity of Nd-doped In_2O_3 porous nanotubes (response value is 46.8) increased 3.5 times while retaining the response and recovery speeds. The response and recovery times of Nd-doped In_2O_3 are 8 s and 22 s, respectively. The ultrahigh response and recovery speed may be attributed to the unique porous structure of ruptured Nd-doped In_2O_3 nanotubes. The cracks and holes on the surface of nanotubes make gas move in and out from the materials much easier and faster, leading to the rapid response and recovery speed. At the same time, this more open structure makes the reaction between a target gas and adsorbed oxygen becomes more intense, which results in the improvement of the sensitivity of gas sensors. In the three dynamic cycles, sensitivity, response and recovery speed remain almost the same, showing the good stability and repeatability of Nd-doped porous In_2O_3 nanotubes.

Sometimes, gas sensors may meet situations of coexistence of multiple gases in practical use, so the selectivity is an important factor for gas sensors. In this experiment, the sensing properties of ruptured

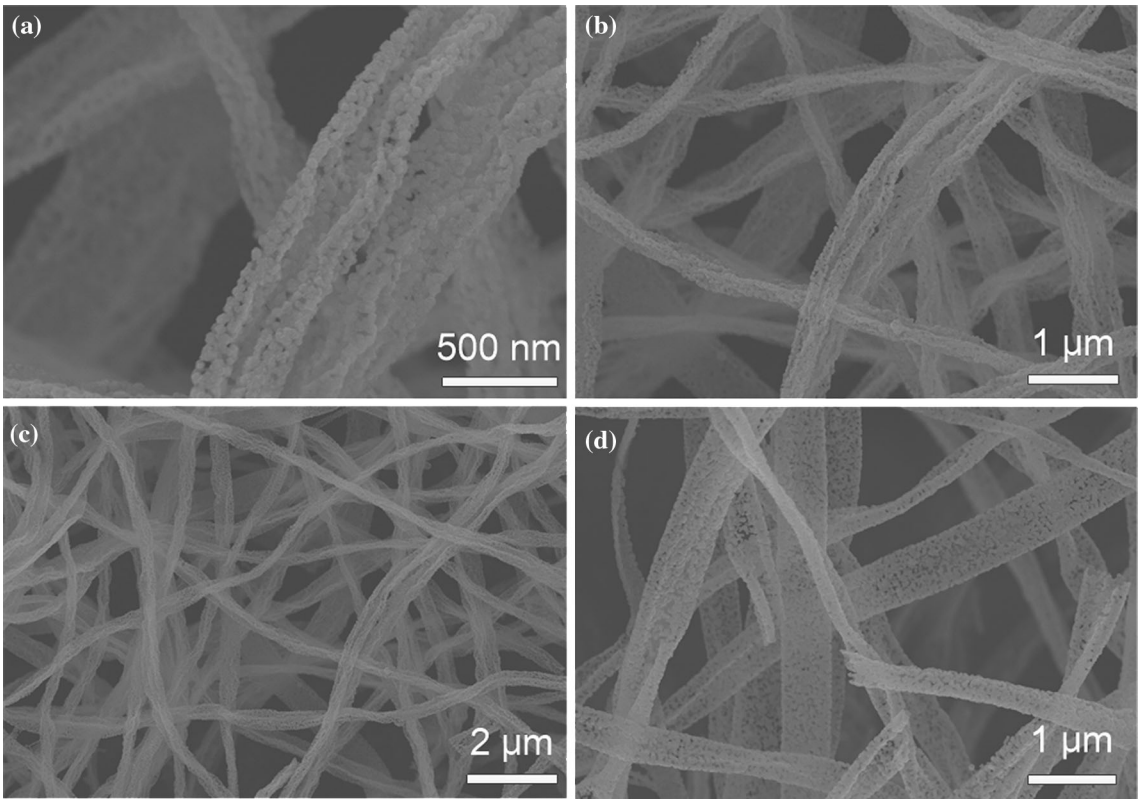

Fig. 3. SEM images of (a, b and c) Nd-doped and (d) pure In_2O_3 porous nanotubes.

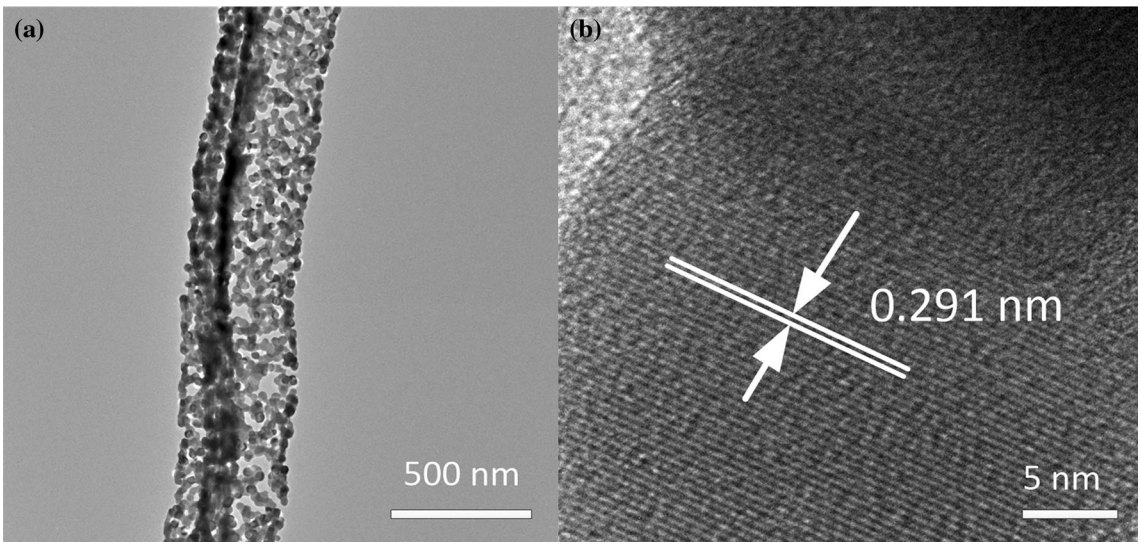

Fig. 4. (a) Typical TEM and (b) HRTEM images of Nd-doped In_2O_3 porous nanotubes.

Nd-doped In_2O_3 porous nanotube sensors to 50 ppm and 100 ppm of several common gases including formaldehyde, toluene, butane, hydrogen, ammonia and carbon monoxide are measured at 240°C. As displayed in Fig. 9, the ruptured Nd-doped In_2O_3 nanotubes show less sensitivity to other gases compared to formaldehyde, indicating the good selectivity of the as-prepared materials.

Figure 10 shows the sensitivity of Nd-doped In_2O_3 porous nanotubes to different concentrations of formaldehyde in 50 days. It can be seen that the sensors almost remain stable during the test, indicating the good long-term stability of Nd-doped In_2O_3 porous nanotubes.

Aiming to show the excellent formaldehyde-sensing properties of the as-prepared Nd-doped In_2O_3

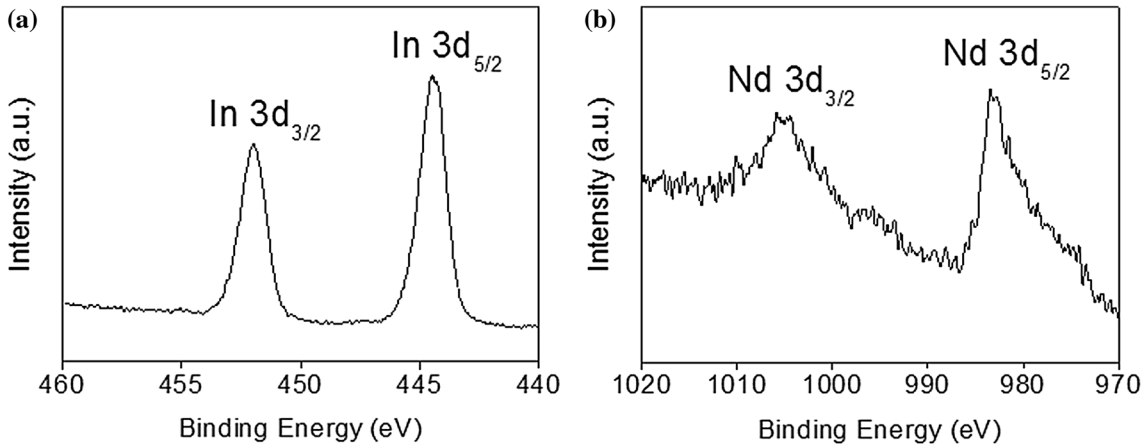

Fig. 5. XPS spectrums of Nd-doped In_2O_3 porous nanotubes, (a) In 3d, (b) Nd 3d.

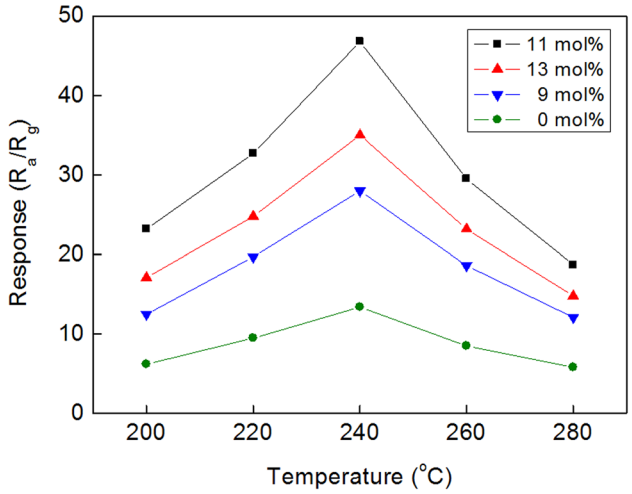

Fig. 6. Response curves of pure, 9 mol.%, 11 mol.%, and 13 mol.% Nd-doped In_2O_3 porous nanotube sensors to 100 ppm formaldehyde at different operating temperatures.

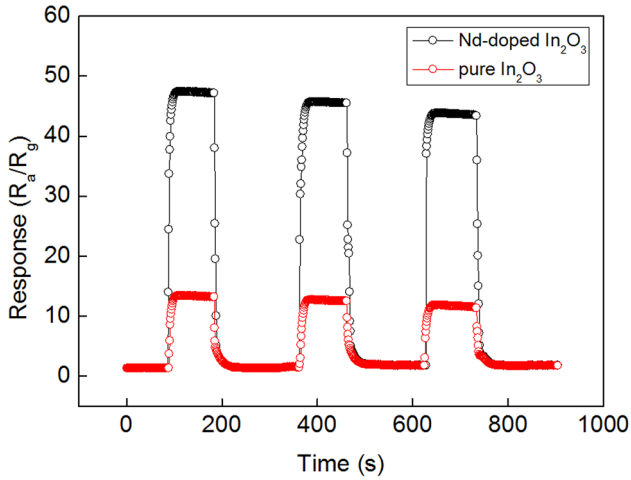

Fig. 8. Response and recovery curves of pure and Nd-doped In_2O_3 porous nanotube sensors to 100 ppm of formaldehyde at 240°C.

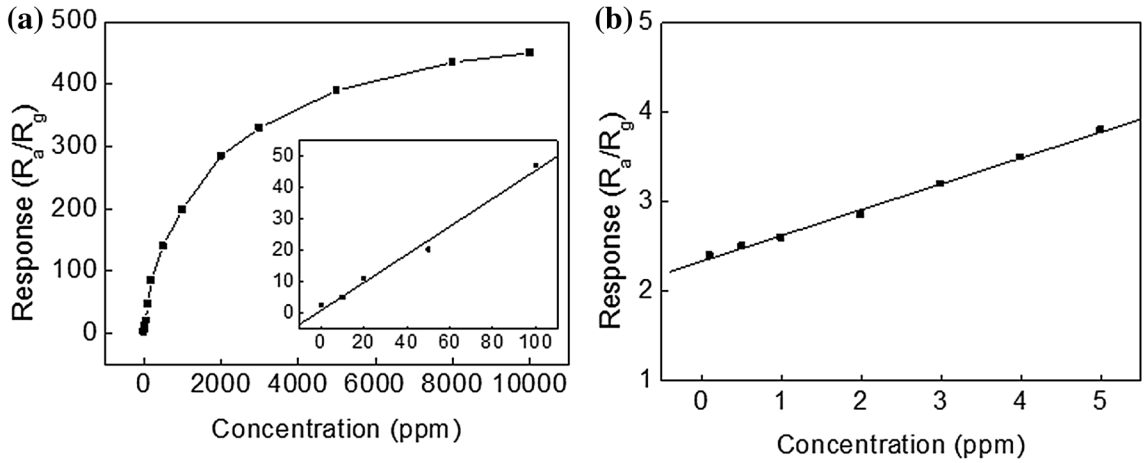

Fig. 7. Response curves of Nd-doped In_2O_3 porous nanotube sensors to (a) different concentrations of formaldehyde (0.1–10000 ppm) and (b) low concentrations (0.1–5 ppm).

porous nanotubes, Table I displays the comparison of Nd-doped In_2O_3 porous nanotubes with other formaldehyde-sensing materials based on In_2O_3. It can be seen that the formaldehyde-sensing property has been improved significantly.

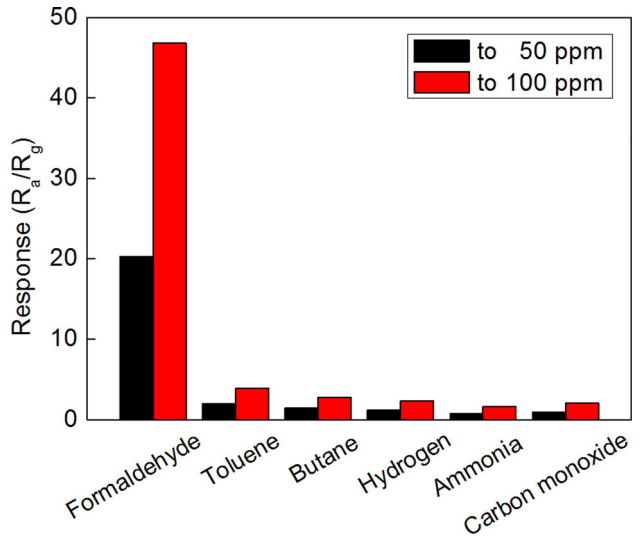

Fig. 9. Responses of ruptured Nd-doped In_2O_3 porous nanotube sensors to different gases at 240°C.

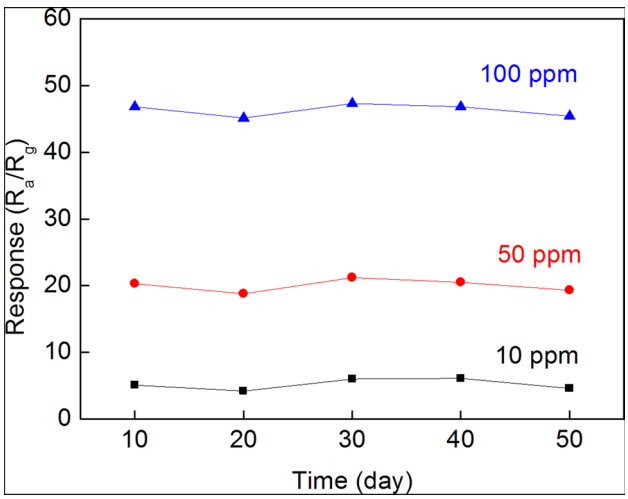

Fig. 10. Long-term stability of Nd-doped In_2O_3 porous nanotube gas sensors.

Gas-Sensing Mechanisms

For gas sensing mechanisms of ruptured Nd-doped In_2O_3 porous nanotubes, the most well-known principle is the change of sensor resistance.[26] When a sensor is exposed in an air condition, O_2 will adsorb on the surface of materials and convert into O^-, O_2^- and O^{2-} and consume electrons from the conduction band of materials.[27] Therefore, the resistance of the sensor decreases as the conductivity declines. However, when a reducing gas such as formaldehyde is introduced, the formaldehyde gas molecules will react with the adsorbed oxygen species and release electrons into the conduction band of materials. Thus, the resistance of the gas sensor decreases.[28] Given the definition of sensitivity of gas sensors ($S = R_a/R_g$), the change in resistance before and after formaldehyde being introduced can be used to detect the concentration of formaldehyde.

Previous studies have demonstrated that the one-dimensional structure of materials can affect gas-sensing performance significantly.[29] The ruptures and pores on the surface of nanotubes can provide easy pathways for gas molecules to penetrate easily into the whole nanotubes. In addition, the ruptures of nanotubes can offer more contact and reaction sites, which will result in more oxygen absorbed on the surface of materials and make the reaction between formaldehyde gas molecules and the absorbed oxygen more violent.[30]

Moreover, the Nd dopant plays another important role in enhancing the gas-sensing performances. It is known that the sensing property is related to the types of sensor (*n*-type or *p*-type), and the electrical properties of the oxide semiconductors are related to the ambient atmosphere. If the conductivity of materials increases with an oxidizing atmosphere, it is called a *p*-type semiconductor; if the conductivity of materials increases with a reducing atmosphere, it is called an *n*-type semiconductor.[31,32] For this experiment, the conductivity of In_2O_3 before and after doping Nd both increase when exposed to the reducing formaldehyde gas; therefore, the In_2O_3 is an *n*-type semiconductor in this test.[12] Many researches have demonstrated that when two semiconducting oxides contact each other, a heterojunction structure will be formed at their interface.[33] Electrons flow from the *n*-type In_2O_3 to the *p*-type

Table I. Comparison of formaldehyde-sensing performance between Nd-doped In_2O_3 porous nanotubes and other In_2O_3-based sensing materials

Gas sensors	Sensitivity	Working temperature/°C	Gas concentration/ppm	Response value	Reference
Nd-doped In_2O_3	R_a/R_g	240	100	46.8	This work
Au@In_2O_3	R_a/R_g	200	100	17	Ref. 22
Sr-doped In_2O_3	R_a/R_g	200	100	9.4	Ref. 23
ZnO-doped In_2O_3	R_a/R_g	260	100	9	Ref. 24
In_2O_3	R_a/R_g	430	100	6.6	Ref. 25

Nd_2O_3[34] while vacancies flow in the opposite direction. At last, the Fermi levels of the two semiconducting oxides in contact reach a balanced state and a depletion layer which hinders electron movement formed at the interface at the same time.[35] Therefore, the resistance of materials in air (R_a) increases significantly after doping with Nd. However, when formaldehyde is introduced, the reaction between formaldehyde gas molecules and the absorbed oxygen will release electrons into the materials and the depletion layer will shrink in this process.[31] Thus, the resistance in the target gas (R_g) decreases. Therefore, the sensitivity of gas sensors (R_a/R_g) increases.

CONCLUSION

In summary, ruptured Nd-doped In_2O_3 porous nanotubes were successfully synthesized via the single-capillary electrospinning method. The formaldehyde-sensing properties were investigated which indicated the unique nanotube structure with ruptures and pores possesses excellent gas-sensing capability. The optimum operating temperature is 240°C for ruptured Nd-doped In_2O_3 porous nanotube sensors, and the response to 100 ppm of formaldehyde is 46.8 at 240°C. The response and recovery times of ruptured Nd-doped In_2O_3 porous nanotubes are 8 s and 22 s, respectively. Furthermore, the lowest detecting limit is 100 ppb with the value of 2.4. In addition, the ruptured Nd-doped In_2O_3 nanotube sensors exhibit good selectivity to formaldehyde and long-term stability. The excellent gas-sensing properties indicate the as-prepared material can be used as a promising candidate for gas sensors in practical applications.

ACKNOWLEDGEMENT

This work has been supported by the Jilin Provincial Science and Technology Department (No. 20140204027GX).

REFERENCES

1. M.A. Omar, H.M. Ahmed, M.A. Hammad, and S.M. Derayea, *Spectrochim. Acta* 472, 135 (2015).
2. K. Zhou, Y. Cheng, H. Yang, C. Gu, Y. Xiao, and M. Zhao, *Sensor. Actuat. B Chem.* 721, 202 (2014).
3. X. Wang, Y. Li, X. Li, J. Yu, S.S. Al-Deyab, and B. Ding, *Sensor. Actuat. B Chem.* 333, 203 (2014).
4. Y. Tang, H. Chen, C. Weng, X. Tang, M. Zhang, and T. Hu, *Spectrochim. Acta* 506, 135 (2015).
5. P. Kar, T. Banerjee, S. Verma, A. Sen, A. Das, B. Ganguly, and H.N. Ghosh, *Phys. Chem. Chem. Phys.* 8192, 14 (2012).
6. A. Brandt and A. Balducci, *J. Power Sources* 44, 230 (2013).
7. A. Afzal, N. Cioffi, L. Sabbatini, and L. Torsi, *Sensor. Actuat. B Chem.* 25, 171–172 (2012).
8. D. Acharyya and P. Bhattacharyya, *Sensor. Actuat. B Chem.* 373, 228 (2016).
9. M. Tiemann, *Chem. Eur. J.* 8376, 13 (2007).
10. L. Wang, X. Luo, X. Zheng, R. Wang, and T. Zhang, *RSC Adv.* 9723, 3 (2013).
11. G.-H. An and H.-J. Ahn, *Carbon* 87, 65 (2013).
12. D. Braun, V. Scherer, C. Janowitz, Z. Galazka, R. Fornari, and R. Manzke, *Phys. Status Solidi A* 59, 211 (2014).
13. L. Xu, B. Dong, Y. Wang, X. Bai, J. Chen, Q. Liu, and H. Song, *J. Phys. Chem. C* 9089, 114 (2010).
14. D.D. Cheng, M.J. Zheng, L.J. Yao, S.H. He, L. Ma, W.Z. Shen, and X.Y. Kong, *Nanotechnology* 425302, 20 (2009).
15. H. Wu, L. Wang, J. Zhou, J. Gao, G. Zhang, S. Xu, Y. Xie, L. Li, and K. Shi, *J. Colloid Interface Sci.* 72, 466 (2016).
16. Y. Lin, H. Ji, Z. Shen, Q. Jia, and D. Wang, *J. Mater. Sci. Mater. Electron.* 2086, 27 (2015).
17. L. Liu, C. Liu, S. Li, L. Wang, H. Shan, X. Zhang, H. Guan, and Z. Liu, *Sensors Actuat. B Chem.* 893, 177 (2013).
18. W. Xu, J. Li, and J. Sun, *RSC Adv.* 81407, 5 (2015).
19. S. Zhang, P. Song, H. Yan, and Q. Wang, *Sensors Actuat. B Chem.* 245, 231 (2016).
20. K. Bouras, G. Schmerber, H. Rinnert, D. Aureau, H. Park, G. Ferblantier, S. Colis, T. Fix, C. Park, W.K. Kim, A. Dinia, and A. Slaoui, *Sol. Energy Mater. Sol. C* 134, 145 (2016).
21. C. Ge, C. Xie, M. Hu, Y. Gui, Z. Bai, and D. Zeng, *Mater. Sci. Eng. B Solid* 43, 141 (2007).
22. X. Li, J. Liu, H. Guo, X. Zhou, C. Wang, P. Sun, X. Hu, and G. Lu, *RSC Adv.* 545, 5 (2015).
23. X. Shen, L. Guo, G. Zhu, C. Xi, Z. Ji, and H. Zhou, *RSC Adv.* 64228, 5 (2015).
24. H. Yang, S. Wang, and Y. Yang, *CrystEngComm* 1135, 14 (2012).
25. Y. Tang and J. Ma, *RSC Adv.* 25692, 4 (2014).
26. C. Zhao, W. Hu, Z. Zhang, J. Zhou, X. Pan, and E. Xie, *Sensors Actuat. B Chem.* 486, 195 (2014).
27. D.D. Vuong, K.Q. Trung, N.H. Hung, N.V. Hieu, and N.D. Chien, *J. Alloys Compd.* 195, 599 (2014).
28. P. Sun, Y. Cai, S. Du, X. Xu, L. You, J. Ma, F. Liu, X. Liang, Y. Sun, and G. Lu, *Sensors Actuat. B Chem.* 336, 182 (2013).
29. C. Liu, X. Chi, X. Liu, and S. Wang, *J. Alloys Compd.* 208, 616 (2014).
30. X. Li, H. Zhang, C. Feng, Y. Sun, J. Ma, C. Wang, and G. Lu, *RSC Adv.* 27552, 4 (2014).
31. D.R. Miller, S.A. Akbar, and P.A. Morris, *Sensors Actuat. B Chem.* 250, 204 (2014).
32. L. Xu, H. Song, B. Dong, Y. Wang, J. Chen, and X. Bai, *Inorg. Chem.* 10590, 49 (2010).
33. W. Tang, J. Wang, P. Yao, and X. Li, *Sensors Actuat. B Chem.* 543, 192 (2014).
34. G. Adachi and N. Imanaka, *Chem. Rev.* 1497, 98 (1998).
35. C. Li, C. Feng, F. Qu, J. Liu, L. Zhu, Y. Lin, Y. Wang, F. Li, J. Zhou, and S. Ruan, *Sensors Actuat. B Chem.* 90, 207 (2015).